Bioconjugate Chemistry

Article

pubs.acs.org/bc

Effective Targeting of DC-SIGN by α-Fucosylamide Functionalized Gold Nanoparticles

Daniela Arosio,*[,†] Fabrizio Chiodo,*[,‡,§] José J. Reina,[∥] Marcello Marelli,[†] Soledad Penadés,[‡,⊥] Yvette van Kooyk,[§] Juan J. Garcia-Vallejo,[§] and Anna Bernardi[†,∥]

[†]CNR-Institute of Molecular Science and Technologies (ISTM), via Golgi 19, I-20133 Milan, Italy

[‡]CIC biomaGUNE, Biofunctional Nanomaterials Unit, Laboratory of GlycoNanotechnology, Paseo Miramón 182, 20009 San Sebastián, Spain

[§]VU University Medical Center, Department of Molecular Cell Biology & Immunology, van der Boechorststraat 7, 1081BT Amsterdam, The Netherlands

[∥]Università degli Studi di Milano, Dipartimento di Chimica, via Golgi 19, I-20133 Milan, Italy

[⊥]CIBER-BBN, Paseo Miramón 182, 20009 San Sebastián, Spain

Supporting Information

ABSTRACT: Dendritic Cells (DCs), the most potent antigen-presenting cells, play a critical role in the detection of invading pathogens, which are recognized also by multiple carbohydrate-specific receptors. Among them, DC-SIGN is one of the best characterized, with high-mannose and Lewis-type glycan specificity. In this study, we present a potent DC-SIGN targeting device developed using gold nanoparticles functionalized with α-fucosyl-β-alanyl amide. The nanoparticles bound to cellular DC-SIGN and induced internalization as effectively as similar particles coated with comparable amounts of Lewis^X oligosaccharide. They were found to be neutral toward dendritic cell maturation and IL-10 production, thus envisaging a possible use as targeted imaging tools and antigen delivery devices.

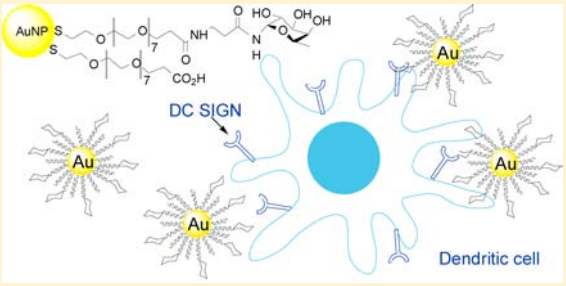

INTRODUCTION

Dendritic cells (DCs) are the most potent antigen-presenting cells and are responsible for the detection of pathogens.[1] DCs are equipped with multiple carbohydrate-specific receptors, called lectins, that recognize a vast array of glycan determinants on both pathogens and host glycoproteins.[2] Ligand recognition often results in internalization and routing to the endolysosomal pathway for processing and antigen presentation. Some lectins, in addition, are able to trigger specific signaling that modulates the maturation and migration of DCs to secondary lymphoid organs for proper stimulation of T cells.[3] Natural carbohydrate ligands for DC lectins include high-mannose *N*-glycans, such as those found on the HIV gp120 envelope-protein, and Lewis-type glycans that also can trigger robust immune responses in humans.[4−6] Targeting antigens to DCs via lectins is a well-known strategy explored in the last 20 years in immunotherapy.[7] Carbohydrate ligands have been used as vehicle to improve DC uptake avoiding adverse immune reactions that may be elicited by monoclonal antibodies.[8] DC-SIGN is one of the best characterized DC lectins with high-mannose and Lewis-type glycan specificity.[9] Targeting DC-SIGN on DCs using multivalent carbohydrate systems is a recent approach that has demonstrated improved uptake, processing, and presentation to antigen-specific T-cells.[10−13] Additionally, DC-SIGN targeting of appropriate imaging reporters may represent a powerful tool to investigate the cellular dynamics of the immune response in lymphoid organs and in peripheral tissues.[14,15]

Our group has recently described the synthesis of a small library of glycomimetic DC-SIGN ligands, characterized by the presence of a β-amino acid tether and a fucosylamide anchor.[16,17] Most of these molecules bind DC-SIGN with an affinity similar to or better than that of the Lewis^X (Le^X) trisaccharide (Galβ1−4[Fucα1−3]GlcNAcβ1), one of its natural fucose-containing ligands.[4,5] In particular, *N*-α-fucosyl-β-alanylamide **1a** (Figure 1), which can be prepared in a single step from fucosyl azide, binds to DC-SIGN with almost the

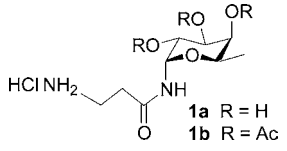

Figure 1. *N*-α-Fucosyl-β-alanylamide **1a**, the monovalent targeting device.

Received: October 13, 2014
Revised: November 5, 2014
Published: November 7, 2014

Scheme 1. Synthesis of the Functionalized AuNPs 5a−d

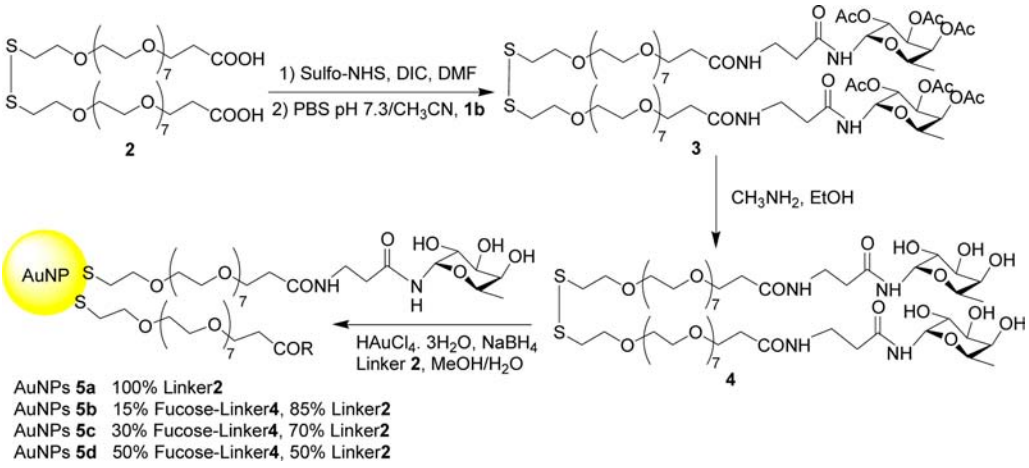

same affinity as Le^X, that has often been used as a DC-SIGN targeting unit in the context of polyvalent constructs.[11−13,18]

Hence, fucosylamide **1a** could clearly represent an inexpensive and effective alternative to the Le^X trisaccharide to build DC-SIGN targeting devices. Indeed, some recent studies indicate that even simple monosaccharides can lead to selective nanoparticle recognition and uptake by immune system cells.[19,20] We therefore synthesized gold nanoparticles (AuNPs) functionalized with multiple copies of **1a** and measured their ability to interact with DC-SIGN on human DCs and to trigger cellular responses following interaction. AuNPs represent an accessible platform for multivalent presentation. These nanomaterials are relatively easy to synthesize and purify, and their size, shape, and coating composition can be finely controlled by choosing the appropriate methodology of preparation.[21−24] Moreover, the globular shape of spherical gold nanoparticles allows a defined and stable 3D presentation of the binding ligand. Finally, gold nanoparticles are considered biocompatible and viable for in vivo applications.[25]

Here, we show that AuNPs bearing 50% of fucosylamide ligand **1a** compete with gp120 on DC-SIGN expressing cells with a potency comparable to that of analogous particles functionalized with much more complex DC-SIGN binding oligosaccharides, such as Le^X. We also show that these particles promote DC-SIGN internalization, do not induce DC maturation, and do not trigger cytokine responses, as demonstrated for some other DC-SIGN ligands.[26] Thus, the AuNPs described in this manuscript can be considered as excellent DC targeting agents and carriers able to deliver antigenic cargo to DCs through DC-SIGN. They appear to lack any immune modulatory capacity, which makes them suitable for use as a basis for antigen-specific vaccination in autoimmunity or cancer, when used with appropriate adjuvants.

RESULTS AND DISCUSSION

The AuNPs were prepared by reduction of tetrachloroauric acid by $NaBH_4$ in the presence of a thiol (or a mixture of thiols), using Brust's method[27] as modified by Penadés (Scheme 1).[28] The required thiols were generated starting from tri-*O*-acetyl-α-L-fucosyl-β-alanine **1b**[29] that was conjugated to commercially available polyethylene glycolic linker **2**, where the disulfide bridge masks the terminal thiol groups. The divalent linker was activated as a bis *N*-hydroxysulfosuccinimide ester and then treated with **1b** in 4:1 phosphate buffer saline (pH 7.3):CH_3CN. The desired bis amide **3** was recovered after purification in 30% yield (unoptimized yield). Acetyl groups removal with 4 M CH_3NH_2 in EtOH afforded the free glycosyl amido-PEG **4**, which was used without further purifications. Direct conjugation of the unprotected fucosylamide **1a** to the activated linker was also attempted; however, it was complicated by formation of an undesired side-product. The masked thiol function of **4** and/or **2** was unmasked in the presence of $HAuCl_4$ by $NaBH_4$ reduction of the disulfide bond. The resulting dark suspension of gold nanoparticles was shaken for ca. 2 h at room temperature and the particles were purified by centrifugal filtration (Vivaspin filters, 10 000 MWCO). Using this protocol, the coating composition of the AuNPs is determined by the mixture of thiols used in the reaction. In particular, 15%, 30%, and 50% mixtures of fucosylamide-derivatized linker **4** and unfunctionalized linker **2** were used, to afford AuNPs **5b−d**, respectively. They were used to investigate the effect of ligand density on AuNP activity. Higher concentrations were not considered, assuming that further increasing the density of the sugar would not improve receptor binding.[30] Control nanoparticles AuNP **5a** were also prepared, bearing no fucose ligands. All the particles synthesized were water-soluble and could be redissolved after lyophilization. They were characterized by high-resolution transmission electron microscopy (HR-TEM) and by ^1H NMR (Supporting Information Figure SI-1−4). The HR-TEM analysis showed uniformly dispersed AuNPs characterized by a very small core (ca. 2 nm) and without signs of aggregation. The ^1H NMR spectrum of fucose functionalized AuNPs confirmed the presence of the sugar on the surface of the nanoparticles, and integrations of the proton signals were in agreement with the expected molar ratio of coating molecules.

To test whether AuNPs were able to target DC-SIGN, we evaluated the binding of soluble DC-SIGN through a solid-phase DC-SIGN binding assay.[31] Flat-bottomed 96-well plates were coated with AuNPs and incubated with a DC-SIGN/Fc chimera for 1 h at 37 °C. After washing, DC-SIGN binding was determined by an ELISA using an antibody against the Fc part of DC-SIGN/Fc. (Le^X-AuNP)[32] carrying 10% of Le^X was used for comparison. The results (Figure 2a) clearly show binding of DC-SIGN to **5d** (carrying 50% of fucosylamide) and to the Le^X-AuNPs in the presence of Ca^{2+} and Mg^{2+}. As a control, AuNP **5a**, carrying only linker **2**, was not recognized by DC-

dx.doi.org/10.1021/bc500467u | Bioconjugate Chem. 2014, 25, 2244−2251

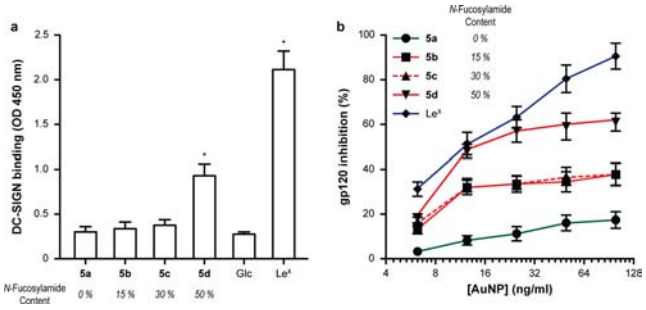

Figure 2. AuNPs **5d** are recognized by DC-SIGN and compete with fluorescently labeled gp120 beads. (a) ELISA plates were coated with AuNPs (15 μg/mL) and their binding to soluble DC-SIGN-Fc was measured in a solid-phase assay. (b) AuNPs (from 12.5 to 100 ng/mL) were coincubated with K-SIGN$_{LL/Y}$ cells in the presence of fluorescently labeled gp120 beads. The AuNPs ability to bind DC-SIGN was measured by FACS as % on inhibition of the gp120 beads-DC-SIGN interaction. Data represent the mean + S. D. of a triplicate experiment. These experiments are representative of at least three independent experiments.

SIGN. In this experiment, no binding was detected for AuNPs **5b−c**, carrying 15% or 30% of fucosyl-amide **1a**.

Because DC-SIGN exists as a tetramer on the membrane of DCs and the soluble DC-SIGN/Fc chimera is a dimer, AuNPs binding was also tested on cellular DC-SIGN, by measuring binding inhibition of fluorescently labeled gp120 beads to a cell line that expresses a mutant form of DC-SIGN unable to internalize (Figure 2b).[33]

The results (Figure 2b) clearly show that both **5d** and Le^X-AuNPs (10% Le^X loading) inhibit gp120 binding to DC-SIGN in a dose-dependent manner with an approximate IC$_{50}$ value around 12 ng/mL. Particles **5c** and **5b** carrying 30% and 15% of fucosyl-amide, respectively, showed a lower but significant ability to interact with cellular DC-SIGN. Control AuNPs carrying 100% of linker **2** (**5a**) showed no binding to cellular DC-SIGN. These results establish AuNPs **5d** as a potent and effective DC-SIGN targeting platform. The different activity of AuNPs **5** relative to the control Le^X-AuNPs (10% Le^X loading) shown in Figure 2 may stem from a number of factors. First of all, it is possible that the presentation of a monosaccharide on the particle is less efficient than the presentation of fucose on a branched trisaccharide. For instance, the monosaccharide ligand can be partially hidden within the PEG layer formed by the linkers. Additionally, and perhaps more relevant, the "inert" ligand in the two AuNPs are significantly different: glucose in the Le^X-AuNPs and carboxylates in AuNPs **5**. Glucose is itself a (weak) DC-SIGN binder,[20,31] while free carboxy groups on our particles do not bind DC-SIGN and may interfere with negatively charged groups (phosphates) on cell membranes. Further optimization of the construct may yield more efficient systems.

It has previously been demonstrated that several pathogens can trigger different cytokine responses through DC-SIGN in a carbohydrate-dependent manner.[26] This mechanism depends on a fine regulatory balance between C-type lectin receptors (CLRs) and Toll-Like Receptors (TLRs) and has sparked the hypothesis that CLRs, and specially DC-SIGN, are immune homeostatic receptors that can be hijacked by pathogens to escape immune surveillance. Differences in the DC-SIGN-dependent signaling responses were described also using multivalent carbohydrate functionalized polymers (PAA-Le^X and PAA-mannose),[26] Le^b glycodendrimers,[11] dendrimers carrying mannoside mimics,[34] or gp120 high-mannoses,[35] indicating that the characterization of the molecular determinants involved in DC-SIGN activation still needs further research. To study the downstream effects of AuNPs **5** on DC, we analyzed the expression of the DC maturation marker CD86 and of the anti-inflammatory cytokine IL-10. CD86 expression was measured by flow cytometry after incubating DCs with AuNPs (1 μg/mL) for 16 h. DCs treated with the TLR4 ligand lipopolysaccharide (LPS 10 ng/mL), a known inducer of DC maturation, were used as a positive control. The results clearly show that neither the AuNPs **5** nor the control Le^X-AuNPs induced CD86 up-regulation at the tested concentration (1 μg/mL) (Figure 3a). DC-SIGN signaling has been reported to synergistically enhance IL-10 expression in the context of simultaneous TLR4 triggering.[26] This was investigated by assaying IL-10 production by DCs after simultaneous incubation with AuNPs **5** (1 μg/mL) and LPS (10 ng/mL). After 16 h, cells were centrifuged and the presence of IL-10 in the supernatant was determined by ELISA (Figure 3b). AuNPs **5** were not able to enhance LPS mediated IL-10 secretion. On the contrary, a glycopeptide dendrimer carrying Le^b (Le^{b}D3, Figure 3b) used as positive control, induced LPS mediated IL-10 up-regulation as previously described.[11] Thus, AuNPs **5** seem to behave as pure targeting devices and be unable to induce DC maturation or to trigger some of the well-known DC-SIGN mediated signaling cascades. In this context, it may be worth noting that AuNPs displaying ManNAc mono- and disaccharides[19] or galactofuranose[20] have been reported to induce significant activation of antigen presenting cells.

Finally, *N*-fucosylamide glyco-nanoparticles **5b−5d** were able to induce DC-SIGN internalization, as measured by imaging flow cytometry (Figure 4). The DC-SIGN binding antibody AZN-D1 was used as positive control (Figure 4a); visualization of the internalized protein was achieved using an anti-DC-SIGN, CRD-independent, antibody (CSRD).[36] Internalization was achieved at 37 °C only and it was directly proportional to the amount of *N*-fucosylamide present on the AuNPs (Figure 4b). DC-SIGN internalization is one of the first events occurring after carbohydrate recognition and it is related to the ability of this lectin to present antigens to the histocompatibility complexes MHC-I and II.[33] The ability of AuNPs **5b−d** to internalize DC-SIGN on DCs suggests that these nanomaterials can be explored for antigen-targeting to DCs.

■ CONCLUSIONS

In this work we developed potent and effective DC-SIGN targeting gold nanoparticles based on *N*-α-fucosyl-β-alanylamide **1a.** The AuNPs **5b−d**, characterized by different sugar densities (15%, 30%, and 50% of fucosylamide) and a diameter of ca. 2 nm, were water-soluble and well dispersed. They were found to bind to DC-SIGN and inhibit gp120 binding to DC-SIGN expressing cells with an efficiency comparable to that of similar polyvalent constructs bearing a comparable load (10%) of the much more complex oligosaccharide Le^X. AuNPs **5b−d** induced DC-SIGN internalization, without triggering DC maturation or the induction of IL-10. Thus, they can be regarded as neutral carriers and DC-SIGN targeting devices. Their use as targeted imaging tools and antigen delivery devices will be explored in due course.

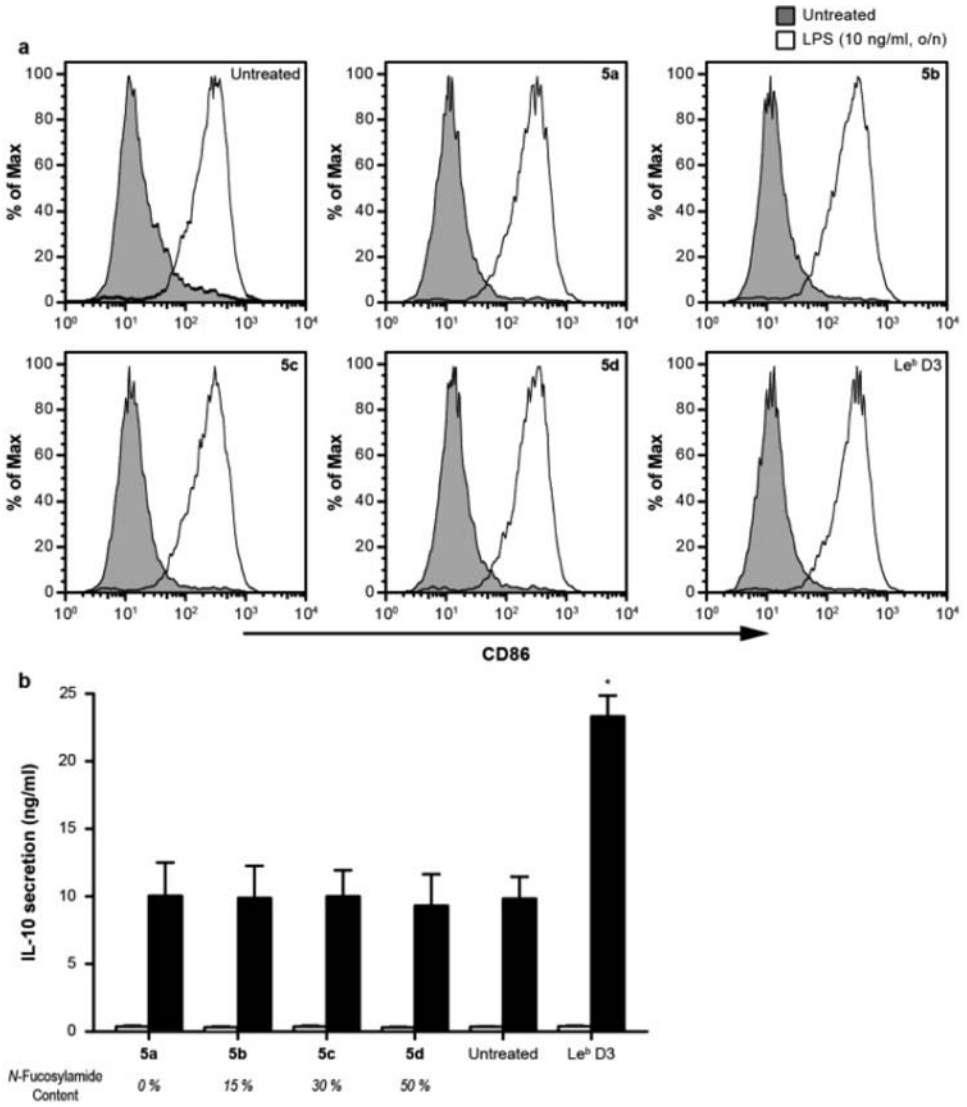

Figure 3. AuNPs **5** do not induce maturation or IL-10 secretion on DCs. (a) Maturation was assessed by CD86 expression human DCs after overnight incubation with AuNPs (gray curves) or LPS (white curve). None of the AuNPs induced DC maturation or altered the typical maturation profile induced by LPS treatment. (b) IL-10 secretion (ng/mL) in human DCs after overnight incubation with AuNPs (white bars) and AuNPs + LPS (dark bars), as measured by ELISA. Le^{b}D3, a Le^b glycopeptide dendrimer,[11] was used as positive control. AuNPs do not show any enhancement in LPS-mediated IL-10 secretion.

EXPERIMENTAL PROCEDURES

Chemistry. *General.* All chemicals and solvents were purchased from Sigma-Aldrich, including linker **2**. They all were of reagent grade and were used without further purification. Solvents were dried by standard procedures and reactions requiring anhydrous conditions were performed under nitrogen atmosphere. *N*-(*β*-Alanyl)-2,3,4-tri-*O*-acetyl-*α*-L-fucopyranosyl amine **1b** was prepared according to a reported procedure.[29] Mass spectra were obtained with an ESI apparatus Bruker Esquire 3000 plus. Thin layer chromatography (TLC) was carried out with precoated Merck F_{254} silica gel plates. Flash chromatography was carried out using the SP1 Flash Purification System by Biotage. ^{1}H and ^{13}C NMR spectra were recorded at 300 K on Bruker AVANCE 400 MHz. Chemical shifts δ are expressed in ppm relative to internal Me_4Si as standard. For transmission electron microscopy (TEM) characterization, a single drop (10 μL) of solution of gold NPs (ca. 0.1 mg/mL in Milli-Q water/ethanol) was placed on a holey carbon copper grid (Electron Microscopy Science) and left to dry in air overnight. The specimens were analyzed by a LIBRA200 EFTEM (ZEISS) with a FEG source and accelerating voltage of 200 kV. The average diameter of the AuNPs was obtained from evaluation of several TEM micrographs, collected spanning large areas of the sample grid, by means of an in-house algorithm for automatic image analysis.

Synthesis of Bis *α*-Fucosyl Amide Conjugated Linker 3. The disulfide linker **2** (from Sigma-Aldrich, 43 mg, 0.047 mmol) and *N*-hydroxysulfosuccinimide sodium salt (25.5 mg, 0.1175 mmol) were dissolved in dry DMF (1.7 mL) and, under nitrogen and at room temperature, *N*,*N*′-diisopropylcarbodiimide (22 μL, 0.141 mmol) was added. The reaction mixture was stirred for 24 h, and then the solvent was removed under reduced pressure. The crude was dissolved in PBS (2.5 mL) and the tetra-*O*-acetyl-*α*-fucosyl-*β*-alanine **1b** (46 mg, 0.1175 mmol) in CH_3CN (0.5 mL) was added. The pH was adjusted to 7.3 by adding NaOH 0.2 N and the reaction mixture was stirred for ca. 24 h monitoring by TLC (CH_3Cl/MeOH 9:1).

dx.doi.org/10.1021/bc500467u | *Bioconjugate Chem.* 2014, 25, 2244−2251

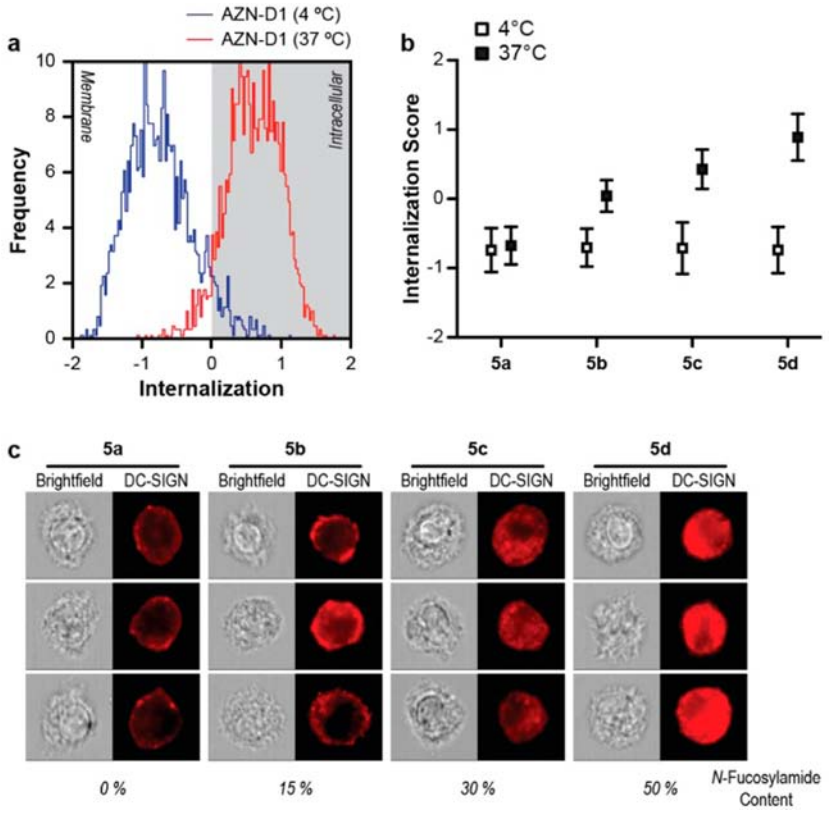

Figure 4. *N*-Fucosylamide glyconanoparticles **5b–d** induce DC-SIGN internalization. (a) DC-SIGN internalization is induced using the CRD-binding antibody AZN-D1. The localization of DC-SIGN is investigated using the CRD-independent antibody CSRD. DC-SIGN internalization is only achieved after DCs have been incubated with AZN-D1 at 37 °C. (b) Only *N*-fucosylamide nanoparticles **5b–d** were able to induce DC-SIGN internalization. Internalization was directly proportional to the amount of *N*-fucosylamide present on the glyconanoparticles. (c) Representative examples of glycan nanoparticles internalization. No internalization was observed with control **5a**.

After reaction completion, the solvent was evaporated under reduced pressure and the crude was purified by automated flash chromatography, eluting with $CHCl_3$/MeOH (gradient from 95:5 to 80:20). The desired product was collected in 30% yield. (white foam). ^{1}H NMR (400 MHz, $CDCl_3$): δ 1.15 (d, 6H, J = 6.1 Hz, CH_3 Fuc), 2.0 (s, 6H, $OCOCH_3$), 2.03 (s, 6H, $OCOCH_3$), 2.18 (s, 6H, $OCOCH_3$), 2.50 (m, 4H, -NHCOCH_2CH$_2$O−), 2.56 (m, 4H, Fuc-NHCOCH_2CH$_2$NH−), 2.88 (t, 4H, -OCH$_2$CH_2SH−), 3.55 (m, 4H, Fuc-NHCOCH$_2$CH_2NH−), 3.60−3.70 (m, 56H, -OCH_2CH_2O−), 3.71−3.78 (m, 8H, -NHCOCH$_2$CH_2O-, -OCH_2CH$_2$SH−), 4.12 (m, 2H, *H*-5 Fuc), 5.28 (m, 2H, *H*-4 Fuc), 5.36 (m, 2H, *H*-2 Fuc), 5.43 (m, 2H, *H*-3 Fuc), 5.93 (m, 2H, *H*-1 Fuc), 7.32 (m, 2H, Fuc-NHCOCH$_2$CH$_2$N*H*-), 8.16 (m, 2H, Fuc-N*H*COCH$_2$CH$_2$NH-). ^{13}C NMR (100.6 MHz, $CDCl_3$): δ 173.7, 172.9, 171.4, 170.8, 170.4, 75.1, 71.6, 71.24, 71.22, 71.16, 71.1, 71.0, 70.9, 70.85, 68.6, 67.8, 67.0, 66.5, 38.9, 37.1, 36.3, 21.4, 21.4, 17.0. MS (ESI$^+$) m/z: 1599.15 $(M+H)^+$, 800.12 $(M+2H)^{2+}$.

Synthesis of 4. The bis α-fucosyl amide conjugated disulfide **3** (22 mg, 0.014 mmol) was dissolved in a 4 M $MeNH_2$ solution in EtOH (420 μL, 1.68 mmol) and stirred at room temperature for 2 h monitoring by TLC (CH_3Cl/MeOH 9:1). After reaction completion, the solvent was evaporated and the crude kept under high vacuum for 6 h, to yield the final product without further purification. 99% yield. (white foam). ^{1}H NMR (400 MHz, D_2O): δ 1.03 (m, 6H, CH_3 Fuc), 2.38 (m, 4H, -NHCOCH_2CH$_2$O−), 2.44 (m, 4H, Fuc-NHCOCH_2CH$_2$NH−), 2.81 (m, 4H, -OCH$_2$CH_2SH−), 3.34 (m, 4H, Fuc-NHCOCH$_2$CH_2NH−), 3.45−3.58 (m, 56H, -OCH_2CH_2O−), 3.59−3.65 (m, 4H, -NHCOH$_2$CH_2O−), 3.66−3.76(m, 10H, *H*-5 Fuc, *H*-4 Fuc, *H*-3 Fuc -OCH_2CH$_2$SH−), 3.86 (m, 2H, *H*-2 Fuc), 4.69 (m, 2H, *H*-1 Fuc). ^{13}C NMR (100.6 MHz, D_2O): δ 175.9, 174.5, 77.2, 72.0, 70.2, 70.1, 70.0, 69.9, 68.9, 68.1, 67.2, 66.5, 37.8, 36.4, 36.2, 35.6, 16.2. MS (ESI$^+$) m/z: 1347.7 $(M+H)^+$, 674.6 $(M+2H)^{2+}$.

General Procedure for Nanoparticle Preparation. The AuNPs were prepared following a described protocol.[28] A 0.012 M (3 equiv) solution of the commercially available linker **2** and of the α-fucosyl amide disulfide **4** (in different proportions) in 1:1 MeOH/H_2O was added to a solution of tetrachloroauric acid (0.025 M, 1 equiv) in water. An aqueous solution of $NaBH_4$ (1 M, 22 equiv) was then added in four portions, with rapid shaking. The black suspension formed was shaken for an additional 2 h at room temperature. After this time the nanoparticles were purified by centrifugal filtration (Vivaspin filters, 10 000 MWCO). The solution was finally lyophilized to afford the desired AuNPs. ^{1}H NMR spectra of the obtained AuNPs were recorded. The particle size distribution of the gold nanoparticles was evaluated from HRTEM micrographs by means of an automatic image analyzer. The average molecular formula of the nanoparticles was calculated on the basis of the average diameter obtained by TEM.[37]

AuNPs ***5a.*** (100% linker **2**): Reaction of **2** (50.0 mg, 0.055 mmol) in MeOH/H_2O 1:1 (9 mL) with $HAuCl_4{\cdot}3H_2O$ (14.6 mg, 0.037 mmol) in 1.5 mL H_2O and $NaBH_4$ (0.8 mL, 1 M) gave AuNPs **5a** (11.6 mg) as a dark-brown powder. TEM average diameter: 2.2 ± 1.5 nm, calculated molecular formula

dx.doi.org/10.1021/bc500467u | *Bioconjugate Chem.* 2014, 25, 2244−2251

and molecular weight: $C_{1656}H_{3496}Au_{309}O_{920}S_{92}$, M.W.: 101 946. ^{1}H NMR (400 MHz, D_2O): δ 2.52−2.62 (m, 2H, HOOCCH_2CH$_2$O−), 3.53−3.80 (m, 32H, CH_2O).

AuNPs **5b**. (15% fucose, 85% linker **2**): Reaction of bis-α-fucosyl-amide derivative **4** (5.4 mg, 0.004 mmol) and linker **2** (17.0 mg, 0.0185 mmol) in MeOH/H_2O 1:1 (4.4 mL) with $HAuCl_4 \cdot 3H_2O$ (7.0 mg, 0.018 mmol) in 720 μL H_2O and $NaBH_4$ (400 μL, 1 M) gave AuNPs **5b** (5.5 mg) as a dark-brown powder. TEM average diameter: 2.81 ± 0.71 nm, calculated molecular formula and molecular weight: $C_{3174}H_{6554}Au_{807}N_{48}O_{1726}S_{163}$, M.W.: 237 194. ^{1}H NMR (400 MHz, D_2O): δ 1.16 (m, 0.45H, CH_3 Fuc), 2.42−2.70 (m, 2.3H, -NHCOCH_2CH$_2$O-Fuc-NHCOCH_2CH$_2$NH-, -HOOCCH_2CH$_2$O), 3.43 (m, 0.3H, Fuc-NHCOCH$_2$CH_2NH−), 3.49−3.92 (m, 32H, CH_2O), 3.93−4.09 (m, 0.45H, *H*-5 Fuc, *H*-4 Fuc, *H*-3 Fuc), 4.12 (m, 0.15H, *H*-2 Fuc), 5.53 (m, 0.15H, *H*-1 Fuc).

AuNPs **5c**. (30% fucose, 70% linker **2**): Reaction of bis-α-fucosyl-amide derivative **4** (11.0 mg, 0.0082 mmol) and linker **2** (17.0 mg, 0.0185) in MeOH/H_2O 1:1 (4.6 mL) with $HAuCl_4 \cdot 3H_2O$ (7.8 mg, 0.0198 mmol) in 730 μL H_2O and $NaBH_4$ (400 μL, 1 M) gave AuNPs **5c** (5.3 mg) as a dark-brown powder. TEM average diameter: 1.92 ± 0.69 nm, calculated molecular formula and molecular weight: $C_{1488}H_{3013}Au_{225}N_{42}O_{794}S_{71}$, M.W.: 80 795. ^{1}H NMR (400 MHz, D_2O): δ 1.15 (m, 0.9H, CH_3 Fuc), 2.40−2.68 (m, 2.6 H, -NHCOCH_2CH$_2$O-Fuc-NHCOCH_2CH$_2$NH-, -HOOCCH_2CH$_2$O), 3.42 (m, 0.6H, Fuc-NHCOCH$_2$CH_2NH−), 3.48−3.92 (m, 32H, CH_2O), 3.93−4.09 (m, 0.9H, *H*-5 Fuc, *H*-4 Fuc, *H*-3 Fuc), 4.13 (m, 0.3H, *H*-2 Fuc), 5.53 (m, 0.3H, *H*-1 Fuc).

AuNPs **5d**. (50% fucose, 50% linker **2**): Reaction of bis-α-fucosyl-amide derivative **4** (23.5 mg, 0.017 mmol) and linker **2** (15.6 mg, 0.017 mmol) in MeOH/H_2O 1:1 (5.6 mL) with $HAuCl_4 \cdot 3H_2O$ (9.0 mg, 0.023 mmol) in 920 μL H_2O and $NaBH_4$ (500 μL, 1 M) gave AuNPs **5d** (8.8 mg) as a dark-brown powder. TEM average diameter: 2.14 ± 0.7 nm, calculated molecular formula and molecular weight: $C_{2098}H_{4148}Au_{314}N_{92}O_{1094}S_{91}$, M.W.: 112 937. ^{1}H NMR (400 MHz, D_2O): δ 1.17 (m, 1.5H, CH_3 Fuc), 2.42−2.70 (m, 3H, -NHCOCH_2CH$_2$O-Fuc-NHCOCH_2CH$_2$NH-, -HOOCCH_2CH$_2$O), 3.46 (m, 1H, Fuc-NHCOCH$_2$CH_2NH−), 3.50−3.92 (m, 32H, CH_2O), 3.93−4.10 (m, 1.5H, *H*-5 Fuc, *H*-4 Fuc, *H*-3 Fuc), 4.12 (m, 0.5H, *H*-2 Fuc), 5.53 (m, 0.5H, *H*-1 Fuc).

Biological Assays. *Cells.* Human monocyte-derived DC were generated from monocytes as previously described.[38] Briefly, monocytes were isolated from the blood of healthy donors (Sanquin, The Netherlands) through a sequential Ficoll/Percoll gradient centrifugation. Isolated monocytes (purity >85%) were cultured in RPMI 1640 (Invitrogen, USA) supplemented with 10% FCS (BioWhittaker, USA), 1000 IU/mL penicillin (BioWhittaker, USA), 1000 IU/mL streptomycin (BioWhittaker, USA), and 2 mM glutamine (BioWhittaker, USA) in the presence of interleukin-4 (IL-4) (500 IU/mL; BioSource, Belgium) and granulocyte-macrophage colony-stimulating factor (GM-CSF) (800 IU/mL; BioSource, Belgium) for 7 days.[39] Monocyte differentiation into DC was confirmed by flow cytometric analysis (FACScan, BD biosciences, USA) of the expression of DC-SIGN using the monoclonal antibody AZN-D1[40] followed by staining with a secondary FITC-labeled antimouse antibody (Zymed, San Francisco, CA).

Stable K562/DC-SIGN$_{LL/Y}$ transfectants[33] were maintained in RPMI 1640 medium containing 10% Fetal Calf Serum 1000 IU/mL penicillin (BioWhittaker, USA), 1000 IU/mL streptomycin (BioWhittaker, USA), and 2 mM glutamine (BioWhittaker, USA). Transfectants were regularly selected using 1 mg/mL Geneticin (Invitrogen, USA). To check for DC-SIGN expression, cells were incubated with primary antibody (AZN-D1) followed by staining with a secondary FITC-labeled antimouse antibody (Zymed, USA) and analyzed by flow cytometry on a FACScan flow cytometer (BD Biosciences, USA). Cell viability was measured using 7-amino actinomycin D (Invitrogen, USA).

DC-SIGN-Fc ELISA.[31] Nunc MaxiSorp plates were coated with 50 μL AuNPs (15 μg/mL in coating buffer, 50 mM Na_2CO_3, pH = 9.7) for 2 h at room temperature. The wells were washed twice with TMS (2 × 200 μL) and blocked with 100 μL TMS with 1% of BSA for 30 min at room temperature. After 1 × 200 μL wash with PBS, the wells were incubated at 37 °C with 50 μL DC-SIGN-Fc (3 μg/mL) in TMS with 1% of BSA for 1 h. The wells were washed four times with TMS (4 × 200 μL) and incubated at room temperature with 50 μL of goat-anti-human HRP (0.8 μg/mL) in TMS with 1% of BSA for 30 min. After four washes with TMS (4 × 200 μL), 100 μL of substrate solution (3,3′,5,5′-tetramethylbenzidine, TMB, in citric/acetate buffer, pH = 4, and H_2O_2) were added and after 4 min at room temperature the reaction was stopped with 50 μL of H_2SO_4 (0.8M) and the plate was read at 450 nm ELISA reader. All the experiments were performed in triplicate. DC-SIGN-Fc consists of the extracellular portion of DC-SIGN (residues 64 to 404) fused at the C-terminus to a human IgG_1/Fc fragment into the Sig-pIgG_1-Fc vector.[41] DC-SIGN/Fc was produced in CHO-K1 cells by cotransfection of DC-SIGN-Sig-pIgG_1 Fc (20 μg) and the pEE14 (5 μg) vector.

Preparation of gp120-Coated Beads. Fluorescently labeled gp120-microbeads were generated in a similar way as described for ICAM-1 beads.[42] In brief, carboxylate-modified TransFluoSpheres (488/645 nm, 1.0 μm, Invitrogen) were coupled to streptavidin (Sigma) followed by incubation with biotinylated F(ab′)2 fragment goat-anti-human IgG Fc fragment (0.5 mg/mL, Jackson Immuno Research) for 2 h at 37 °C. Next, the beads were washed and coupled to purified HIV-1 gp120-Fc protein (1 μg/mL) by an overnight incubation at 4 °C. After extensive washing in ice-cold PBS, beads were reconstituted in 50 μL of PBS.

Gp120 Binding Assay. Stable K562/DC-SIGN$_{LL/Y}$ transfectants (5 × 10^4 per well) were incubated with gold nanoparticles for 45 min at 37 °C. Next, gp120 fluorescent beads were added to the cells and incubated for another 45 min at 4 °C. The percentage of gp120 beads-positive cells was analyzed by flow cytometry (BD Biosciences, USA).

Flow Cytometry Analysis of DC Surface Molecules and Cytokine Production. Suspensions of 100 μL immature DCs (1 × 10^6 cells/mL) were stimulated by addition of AuNPs (1 μg/mL) for 16−20 h at 37 °C in the presence of 5% CO_2. 10 ng/mL LPS (*E. coli*, Sigma-Aldrich) served as a control. Cells were then collected by centrifugation, washed with 1% BSA in phosphate-buffered saline and incubated with mouse anti-human CD86 conjugated with phycoerythrin (PE, BD Pharmingen, San Diego, CA). After 30 min incubation at 4 °C, cells were analyzed using a flow cytometer (FACS Calibur, BD Biosciences, USA).

IL-10 ELISA. For the detection of IL-10, culture supernatants were harvested 24 h after DC stimulation and frozen at

−80 °C until analysis. Cytokines were measured by ELISA using antibody pairs from eBioscience (The Netherlands) and according to manufacturer's protocols.

Internalization Assay. DCs were incubated in the presence of gold nanoparticles at either 4 or 37 °C for 60 min. Cells were then washed, fixed, and stained against DC-SIGN using the polyclonal antibody CSRD,[36] and an AF488-labeled goat-anti-rabbit antibody, and then prepared for acquisition on the ImageStreamX (Amnis corp., Seattle) imaging flow cytometer. The following laser powers were used: 488 nm at 20 mW and 785 nm at 4.5 mW. Brightfield illumination was set at 800 mW before the acquisition of each sample. Brightfield images were collected in channels 1 and 9. Channels 2 (Atto488) and 6 (granularity) were habilitated for the internalization assay. Cells were acquired at 60× magnification and on the basis of their area (area = the number of pixels in an image reported in square microns). Minimum area for acquisition was set to 50 pixels. A minimum of 15×10^3 cells was acquired per sample at a flow rate ranging between 50 and 100 cells/s. At least 2×10^3 cells were acquired from single stained samples to allow for compensation. Compensation samples were acquired with all channels habilitated and with the brightfield illumination and the 785 nm laser switched off. A minimum of 5×10^3 cells from the single stained samples were acquired with the same settings as experimental samples to control for over/under compensation. Analysis was performed using the IDEAS v 6.0 software (Amnis corp., Seattle) as previously described.[43] The internalization score is a log-scaled ratio of the intensity inside the cell (intracellular mask) with respect to the intensity of the entire cell. Cells that have internalized antigen typically have positive scores, while cells that show the antigen still on the membrane have negative scores. Cells with scores around 0 have similar amounts of antigen on the membrane and in intracellular compartments.

■ ASSOCIATED CONTENT

Supporting Information

Characterization of fucosylamide-derivatized linker **4**. Table with tentative molecular formula. TEM micrographs, size-distribution histograms and ^{1}H NMR spectra of gold nanoparticles. This material is available free of charge via the Internet at http://pubs.acs.org.

■ AUTHOR INFORMATION

Corresponding Authors

*E-mail: daniela.arosio@istm.cnr.it.
*E-mail: f.chiodo@lumc.nl.

Present Address

Fabrizio Chiodo, Department of Parasitology, Leiden University Medical Center, Albinusdreef 2, 2333 ZA Leiden, The Netherlands.

Notes

The authors declare no competing financial interest.

■ ACKNOWLEDGMENTS

This work was financially supported by the European Union (contract Carmusys FP7-PEOPLE-213592) and by project RSPPTECH (CNR and Regione Lombardia convenzione operativa no 18095/RCC) and by the Spanish Ministry of Science and Innovation, MICINN (Grant CTQ2011-27268). F. C. was supported by MICINN (Grant No. CTQ2008-04638). J. J. G.-V. is supported by the Dutch Asthma Foundation (grant 3.2.10.040).

■ REFERENCES

(1) Steinman, R. M., and Banchereau, J. (2007) Taking dendritic cells into medicine. *Nature 449*, 419−426.

(2) García-Vallejo, J. J., and van Kooyk (2009) Y. Endogenous ligands for C-type lectin receptors: the true regulators of immune homeostasis. *Immunol. Rev. 230*, 22−37.

(3) Geijtenbeek, T. B. H., and Gringhuis, S. I. (2009) Signalling through C-type lectin receptors: shaping immune responses. *Nat. Rev. Immunol. 9*, 465−479.

(4) Appelmelk, B. J., van Die, I., van Vliet, S. J., Vanedenbroucke-Grauls, C. M., Geijtenbeek, T. B., and van Kooyk, Y. (2003) Cutting edge: carbohydrate profiling identifies new pathogens that interact with dendritic cell-specific ICAM-3-grabbing nonintegrin on dendritic cells. *J. Immunol. 170*, 1635−1639.

(5) van Liempt, E., Bank, C. M., Mehta, P., Garciá-Vallejo, J. J., Kawar, Z. S., Geyer, R., Alvarez, R. A., Cummings, R. D., van Kooyk, Y., and van Die, I. (2006) Specificity of DC-SIGN for mannose- and fucose-containing glycans. *FEBS Lett. 580*, 6123−6131.

(6) Everts, B., Smits, H. H., Hokke, C. H., and Yazdanbakhsh, M. (2010) Helminths and dendritic cells: sensing and regulating via pattern recognition receptors, Th2 and Treg responses. *Eur. J. Immunol. 40*, 1525−1537.

(7) For a seminal example involving the DEC-205 receptor see: Hawiger, D., Inaba, K., Dorsett, Y., Guo, M., Mahnke, K., Rivera, M., Ravetch, J. V., Steinman, R. M., and Nussenzweig, M. C. (2001) Dendritic cells induce peripheral T cell unresponsiveness under steady state conditions in vivo. *J. Exp. Med. 194*, 769−779.

(8) Wang, J., Zou, Z. H., Xia, H. L., He, J. X., Zhong, N. S., and Tao, A. L. (2012) Strengths and weaknesses of immunotherapy for advanced non-small-cell lung cancer: a meta-analysis of 12 randomized controlled trials. *PLoS One 7*, e32695.

(9) Geijtenbeek, T. B. H., Kwon, D. S., Torensma, R., van Vliet, S. J., van Duijnhoven, G. C. F., Middel, J., Cornelissen, I. L. M. H. A., Nottet, H. S. L. M., KewalRamani, V. N., Littman, D. R., Figdor, C. G., and van Kooyk, Y. (2000) DC-SIGN, a dendritic cell-specific HIV-1-binding protein that enhances trans-infection of T cells. *Cell 100*, 587−597.

(10) Arnáiz, B., Martínez-Ávila, O., Falcon-Perez, J. M., and Penadés, S. (2012) Cellular uptake of gold nanoparticles bearing HIV gp120 oligomannosides. *Bioconjugate Chem. 23*, 814−825.

(11) García-Vallejo, J. J., Ambrosini, M., Overbeek, A., van Riel, W. E., Bloem, K., Unger, W. W., Chiodo, F., Bolscher, J. G., Nazmi, K., Kalay, H., and van Kooyk, Y. (2013) Multivalent glycopeptide dendrimers for the targeted delivery of antigens to dendritic cells. *Mol. Immunol. 53*, 387−397.

(12) Singh, S. K., Stephani, J., Schaefer, M., Kalay, H., García-Vallejo, J. J., den Haan, J., Saeland, E., Sparwasser, T., and van Kooyk, Y. (2009) Targeting glycan modified OVA to murine DC-SIGN transgenic dendritic cells enhances MHC class I and II presentation. *Mol. Immunol. 47*, 164−174.

(13) Unger, W. W. J., van Beelen, A. J., Bruijns, S. C., Joshi, M., Fehres, C. M., van Bloois, L., Verstege, M. I., Ambrosiani, M., Kalay, H., Nazmi, K., Bolscher, J. G., Hooijberg, E., de Gruijl, T. D., Storm, G., and van Kooyk, Y. (2012) Glycan-modified liposomes boost CD4+ and CD8+ T-cell responses by targeting DC-SIGN on dendritic cells. *J. Controlled Release 160*, 88−95.

(14) Germani, R. N., Robey, E. A., and Cahalan, M. D. (2012) A decade of imaging cellular motility and interaction dynamics in the immune system. *Science 336*, 1676−1681.

(15) Cruz, L. J., Tacken, P. J., Bonetto, F., Buschow, S. I., Croes, H. J., Wijers, M., de Vries, I. J., and Figdor, C. G. (2011) Multimodal imaging of nanovaccine carriers targeted to human dendritic cells. *Mol. Pharmaceutics 8*, 520−531.

(16) Andreini, M., Doknic, D., Sutkeviciute, I., Reina, J. J., Duan, J., Chabrol, E., Thepaut, M., Moroni, E., Doro, F., Belvisi, L., Weiser, J., Rojo, J., Fieschi, F., and Bernardi, A. (2011) Second generation of

fucose-based DC-SIGN ligands: affinity improvement and specificity versus Langerin. *Org. Biomol. Chem. 9*, 5778−5786.
(17) Doknic, D., Abramo, M., Sutkeviciute, I., Reinhardt, A., Guzzi, C., Schlegel, M. K., Potenza, D., Nieto, P. M., Fieschi, F., Seeberger, P. H., and Bernardi, A. (2013) Synthesis and characterization of linker-armed fucose-based glycomimetics. *Eur. J. Org. Chem.*, 5303−5314.
(18) Rouhanifard, S. H., Xie, R., Zhang, G., Sun, X., Chen, X., and Wu, P. (2012) Detection and isolation of dendritic cells using Lewis X-functionalized magnetic nanoparticles. *Biomacromolecules 13*, 3039−3045.
(19) Fallarini, S., Paoletti, T., Orsi Battaglini, C., Ronchi, P., Lay, L., Bonomi, R., Jha, S., Mancin, F., Scrimin, P., and Lombardi, G. (2013) Factors affecting T cell responses induced by fully synthetic glyco-gold-nanoparticles. *Nanoscale 5*, 390−400.
(20) Chiodo, F., Marradi, M., Park, J., Ram, A. F. J., Penades, S., van Die, I., and Tefsen, B. (2014) Galactofuranose-coated gold nanoparticles elicit a proinflammatory response in human monocyte-derived dendritic cells and are recognized by DC-SIGN. *ACS Chem. Biol. 9*, 383−389.
(21) Marradi, M., Chiodo, F., García, I., and Penadés, S. (2013) Glyconanoparticles as multifunctional and multimodal carbohydrate systems. *Chem. Soc. Rev. 42*, 4728−4745.
(22) Llevot, A., and Astruc, D. (2012) Applications of vectorized gold nanoparticles to the diagnosis and therapy of cancer. *Chem. Soc. Rev. 41*, 242−257.
(23) Boisselier, E., and Astruc, D. (2009) Gold nanoparticles in nanomedicine: preparations, imaging, diagnostics, therapies and toxicity. *Chem. Soc. Rev. 38*, 1759−1782.
(24) Arvizio, R., Bhattacharya, R., and Mukherjee, P. (2010) Gold nanoparticles: opportunities and challenges in nanomedicine. *Expert Opin. Drug Delivery 7*, 753−763.
(25) Duncan, B., Kim, C., and Rotello, V. M. (2010) Gold nanoparticle platforms as drug and biomacromolecule delivery systems. *J. Controlled Release 148*, 122−127.
(26) Gringhuis, S. I., den Dunnen, J., Litjens, M., van der Vlist, M., and Geijtenbeek, T. B. (2009) Carbohydrate-specific signaling through the DC-SIGN signalosome tailors immunity to Mycobacterium tuberculosis, HIV-1 and Helicobacter pylori. *Nat. Immunol. 10*, 1081−1088.
(27) Brust, M., Walker, M., Bethell, D., Schiffrin, D. J., and Whyman, R. (1994) Synthesis of thiol-derivatised gold nanoparticles in a two-phase liquid-liquid system. *J. Chem. Soc., Chem. Commun.*, 801−802.
(28) Barrientos, A. G., de la Fuente, J. M., Rojas, T. C., Fernandez, A., and Penades, S. (2003) Gold glyconanoparticles: synthetic polyvalent ligands mimicking glycocalyx-like surfaces as tools for glycobiological studies. *Chem.—Eur. J. 9*, 1909−1921.
(29) Andreini, M., Anderluh, M., Audfray, A., Bernardi, A., and Imberty, A. (2010) Monovalent and bivalent N-fucosyl amides as high affinity ligands for Pseudomonas aeruginosa PA-IIL lectin. *Carb. Res. 345*, 1400−1407.
(30) Martinez-Avila, O., Hijazi, K., Marradi, M., Clavel, C., Campion, C., Kelly, C., and Penades, S. (2009) Gold manno-glyconanoparticles: multivalent systems to block HIV-1 gp120 binding to the lectin DC-SIGN. *Chem.—Eur. J. 15*, 9874−9888.
(31) Chiodo, F., Marradi, M., Tefsen, B., Snippe, H., van Die, I., and Penadés, S. (2013) High sensitive detection of carbohydrate binding proteins in an ELISA-solid phase assay based on multivalent glyconanoparticles. *PLoS One 8*, e73027.
(32) de La Fuente, J. M., Barrientos, A. G., Rojas, T. C., Rojo, J., Cañada, J., Fernández, A., and Penadés, S. (2001) Gold glyconanoparticles as water-soluble polyvalent models to study carbohydrate interactions. *Angew. Chem., Int. Ed. 40*, 2257−2261.
(33) Engering, A., Geijtenbeek, T. B., van Vliet, S. J., Wijers, M., van Liempt, E., Demaurex, N., Lanzavecchia, A., Fransen, J., Figdor, C. G., Piguet, V., and van Kooyk, Y. (2002) The dendritic cell-specific adhesion receptor DC-SIGN internalizes antigen for presentation to T cells. *J. Immunol. 168*, 2118−2126.
(34) Berzi, A., Varga, N., Sattin, S., Antonazzo, P., Biasin, M., Cetin, I., Trabattoni, D., Bernardi, A., and Clerici, M. (2014) Pseudo-mannosylated DC-SIGN ligands as potential adjuvants for HIV vaccines. *Viruses 6*, 391−403.
(35) Shan, M., Klasse, P. J., Banerjee, K., Dey, A. K., Iyer, S. P., Dionisio, R., Charles, D., Campbell-Gardener, L., Olson, W. C., Sanders, R. W., and Moore, J. P. (2007) HIV-1 gp120 mannoses induce immunosuppressive responses from dendritic cells. *PLoS Pathog. 3*, e169.
(36) Engering, A., van Vliet, S. J., Hebeda, K., Jackson, D. G., Prevo, R., Singh, S. K., Geijtenbeek, T. B. H., van Krieken, H., and van Kooyk, Y. (2004) Dynamic populations of dendritic cell-specific ICAM-3 grabbing nonintegrin-positive immature dendritic cells and liver/lymph node-specific ICAM-3 grabbing nonintegrin-positive endothelial cells in the outer zones of the paracortex of human lymph nodes. *Am. J. Pathol. 164*, 1587−1595.
(37) Hostetler, M. J., Wingate, J. E., Zhong, C.-J., Harris, J. E., Vachet, R. W., Clark, M. R., Londono, J. D., Green, S. J., Stokes, J. J., Wignall, G. D., Glish, G. L., Porter, M. D., Evans, N. D., and Murray, R. W. (1998) Alkanethiolate gold cluster molecules with core diameters from 1.5 to 5.2 nm: core and monolayer properties as a function of core size. *Langmuir 14*, 17−30.
(38) Sallusto, F., Cella, M., Danieli, C., and Lanzavecchia, A. (1995) Dendritic cells use macropinocytosis and the mannose receptor to concentrate macromolecules in the major histocompatibility complex class II compartment: downregulation by cytokines and bacterial products. *J. Exp. Med. 182*, 389−400.
(39) Sallusto, F., and Lanzavecchia, A. (1994) Efficient presentation of soluble antigen by cultured human dendritic cells is maintained by granulocyte/macrophage colony-stimulating factor plus interleukin 4 and downregulated by tumor necrosis factor alpha. *J. Exp. Med. 179*, 1109−1118.
(40) Geijtenbeek, T. B., Torensma, R., van Vliet, S. J., van Duijnhoven, G. C., Adema, G. J., van Kooyk, Y., and Figdor, C. G. (2000) Identification of DC-SIGN, a novel dendritic cell-specific ICAM-3 receptor that supports primary immune responses. *Cell 100*, 575−585.
(41) Fawcett, J., Holness, C. L. L., Needham, L. A., Turley, H., Gattert, K. C., Mason, D. Y., and Simmons, D. L. (1992) Molecular cloning of ICAM-3, a third ligand for LFA-1, constitutively expressed on resting leukocytes. *Nature 360*, 481−484.
(42) Geijtenbeek, T. B. H., van Kooyk, Y., van Vliet, S. J., Renes, M. H., Raymakers, R. A. P., and Figdor, C. G. (1999) High frequency of adhesion defects in B-lineage acute lymphoblastic leukemia. *Blood 94*, 754−764.
(43) Garcia-Vallejo, J. J., Koning, N., Ambrosiani, M., Kalay, H., Vuist, I., Sarrami-Forooshani, R., Geijtenbeek, T. B. H., and van Kooyk, Y. (2013) Glycodendrimers prevent HIV transmission via DC-SIGN on dendritic cells. *Int. Immunol. 2*, 221−233.